Tracking UWB Monocycles in IEEE 802.15 Multi-path Channels

Chee-Cheon Chui and Robert A. Scholtz[1]
UltRa Lab, Communication Sciences Institute
University of Southern California
Los Angeles, CA 90089-2565

Abstract - **This paper analyzes the variance of the timing error at the output of the timing error detector as a result of multipath effects. While [3] and others have examined similar channel impairments on spread spectrum CDMA systems employing rake receiver with early-late timing detector, it is not known how severe multipath will affect UWB tracking loop. An UWB system transmitting impulses generally has considerably larger bandwidth and operates at higher frequencies mandated by FCC. Also, UWB impulse system utilizes short duration monocycles separated in time by the frame period unlike conventional continuous time signal. Thus, it has the advantage of being able to resolve more closely spaced multipaths than most other existing spread spectrum systems. Indeed, our analysis shows that, assuming clusters are well separated, and for channel parameters reported in [2], the self-interference due to rays in the same cluster may not be 'harmful' for most applications.**

I. Introduction

The effect of multipath frequency selective fading on time tracking error was studied in [3][4] and references therein. The application of these works is in rake receivers for DS-CDMA systems and assumes early-late timing error detector as the basic building block. Reference [3] summarizes that either interference cancellation or interference minimization is used to mitigate the multipath self-interference in the timing error detector. The multipath self-interference appears as low frequency interference in the tracking loop and cannot be removed using high pass filtering. The detrimental effects of this low frequency interference on system performance are said to be significant and warrant additional signal processing, either before or after the timing error detector.

However, given an UWB system's ability to resolve closely spaced multipath, it is of interest to understand how, with the larger bandwidth allocated by FCC and operating in the modified SV channel model proposed by the IEEE 802.15 working group, the performance of the error tracking timing detector is affected. Also, the targeted application here is ranging using UWB impulse signals.

The analysis detailed herein uses the multipath channel model proposed by the IEEE 802.15 working group for wireless indoor UWB applications. We modeled the received UWB monocycles as the n^{th} order (n>0) derivative of the Gaussian function and formulated the variance of the timing error detector output assuming we are tracking the first ray of an arbitrary l^{th} multipath cluster. The detector output variance can be written in two separate parts: variance of the first ray with additive white Gaussian noise (AWGN) and the variance attributed to self-interference from the multipath components. The variance associated with the first ray is bounded by the Cramer-Rao bound. An expression is then derived for the variance due to the second ray in the cluster. Using a 8th order Gaussian derivative monocycle that fits into the FCC indoor spectral mask, we show that indeed the additional variance is small for channel parameters reported in IEEE 802.15 report [2].

[1]This work was supported in part by a MURI Project under Contract DAAD 19-01-1-0477 from the US Army Research Office. Chee-Cheon Chui's postgraduate study in USC is supported by DSO National Laboratories, Singapore.

II. UWB Multi-path channel model

The UWB multi-path channel model is adopted from the modified SV model described by the IEEE 802.15 working group [2]. It describes a UWB multipath channel consisting of clusters of 'rays' arriving at the receiver. The channel impulse response consists of Dirac delta functions spaced according to the inter-rays arrival time and rays are group into cluster. The rays are attenuated by exponential decaying factor with log-normal shadowing on the profile of the channel impulse response. The discrete time channel impulse response is of the form:

$$h(t) = \chi \sum_{l=0}^{L} \sum_{k=0}^{K} \alpha_{k,l} \cdot \delta(t - T_l - \tau_{k,l}) \qquad (1)$$

where χ represents log-normal shadowing, $\alpha_{k,l}$ is the multipath gain coefficient, T_l is the delay of the l^{th} cluster and $\tau_{k,l}$ the delay of the k^{th} multipath component relative to the l^{th} cluster arrival time. The cluster and ray arrival rate are Λ and λ respectively. The inter-arrival time of the cluster and rays within each cluster are modelled using exponential distributions. Specifically, we have for $\tau_{k,l}$:

$$P(\tau_{k,l} \mid \tau_{(k-1),l}) = \lambda \cdot e^{-\lambda(\tau_{k,l} - \tau_{k-1,l})}, \quad k > 0 . \qquad (2)$$

As the first ray in the cluster marks the cluster arrival, we have $\tau_{o,l} = 0$. The channel coefficients $\alpha_{k,l}$ is given by

$$\alpha_{k,l} = \rho_{k,l} \cdot \xi_l \cdot \beta_{k,l} . \qquad (3)$$

Signal inversion due to reflections is modelled via $\rho_{k,l}$, which is distributed equi-probably over ±1. The factors ξ_l and $\beta_{k,l}$ denotes fading associated with the l^{th} cluster and the k^{th}

ray of the l^{th} cluster respectively. It is further defined in [2] that

$$E\left\{\left|\xi_l \beta_{k,l}\right|^2\right\} = \Omega_o e^{-T_l/\Gamma} e^{-\tau_{k,l}/\gamma} \quad (4)$$

where Ω_o is the mean energy of the first path of the first cluster. The cluster and ray attenuation factors are Γ and γ respectively.

III. DETECTOR OUTPUT

In [1], we have described a correlation timing detector as shown in Fig. 1. It correlates the received UWB impulses with the reference signal generated at and timed by the local voltage control oscillator (VCO) of the receiver. The timing detector operates nominally at symbol/pulse repetition rate, i.e., the timing error is computed, and the control signal to the VCO is updated only once per pulse repetition period (or per received UWB impulse). The output of the timing detector will be a signal proportional in magnitude and of the same sign (for positive loop gain) as the timing difference between the received signal and the locally generated reference signal. For one correlation period of the detector, we can write,

$$x = K_D \cdot g(\varepsilon) + K_D \cdot n' \quad (5)$$

where
$$g(\varepsilon) = A_s A_r \int_{-\infty}^{\infty} q(t) r(t+\varepsilon) dt \quad (6)$$

and
$$n' = A_r \int_{-T_D+\hat{\xi}}^{T_D+\hat{\xi}} n(t) r(t-\hat{\xi}) dt \,. \quad (7)$$

The AWGN noise *n(t)* has zero mean and one-sided power spectral density N_o. The timing difference between the received and reference signal is ε and $\hat{\xi}$ denotes the estimate of the delay of the received monocycle. The received and reference monocycle waveform are *q(t)* and *r(t)* respectively and their energies A_s^2 and A_r^2. We assume *q(t)* and *r(t)* are limited in time, i.e., $q(t) \approx 0$ and $r(t) \approx 0$ for $|t| > T_D$. The detector gain K_D has unit of seconds/volts^2 and is designed to make the slope of the open-loop S-function at $\varepsilon = 0$ to be 1 and fixed as a constant once A_s, A_r, $q(t)$ and $r(t)$ have been determined. It has the form:

$$K_D = 1 \Big/ \left. \frac{d}{d\varepsilon} A_s A_r \int_{-\infty}^{\infty} q(t) r(t+\varepsilon) dt \right|_{\varepsilon=0} \,. \quad (8)$$

We assume that we are tracking the first ray of the (arbitrary) l^{th} multipath cluster. Then, if $\varepsilon = 0$, the first ray is 'in-phase' with the reference signal. However, due to the presence of multipath in the channel, the detector output x will not be zero when the receiver aligned with the first ray of the cluster. The tracking loop will then seek to drive the detector output to zero. Thus there is an offset/bias on the delay estimate. This offset corresponds to the deviation from the actual time-of-arrival of the first ray of the cluster due to presence of multipath in the channel. The conventional detector as shown in Fig. 1 is not capable of correcting this offset in the delay estimate.

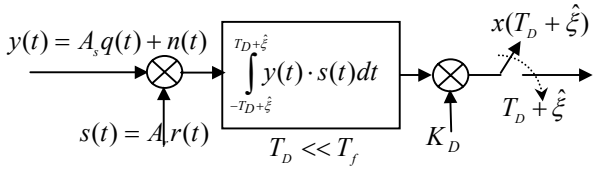

Figure 1: Illustration of correlator timing error detector. The input signal and the reference signal is multiplied and integrated over a period of $2T_D$ to obtain the timing error output. The pulse repetition period is T_f.

In subsequent analysis, we assume, in the presence of multipaths, the received signal is given as:

$$y(t) = A_t \chi \sum_l \sum_k \alpha_{k,l} q(t - T_l - \tau_{k,l}) + n(t) \quad (9)$$

and A_t is the amplitude of the transmitted monocycle. The output of the detector, in the absence of noise, is then presented as:

$$K_D \cdot g(\varepsilon) = K_D \chi A_t A_r \sum_l \sum_k \alpha_{k,l} \int_{-\infty}^{\infty} q(t - T_l - \tau_{k,l}) r(t+\varepsilon) dt \,. \quad (10)$$

In the modified SV channel model for UWB systems [2], the signal inversion coefficient $\rho_{k,l}$ is statistically independent and has zero mean. As a result:

$$E\{K_D \cdot g(\varepsilon)\} = 0 \quad (11)$$

and the variance of the sum of (10) is the sum of the variances. Thus the variance of the detector output is computed as:

$$\begin{aligned} K_D^2 E\{g^2(\varepsilon)\} &= K_D^2 \cdot A_t^2 A_r^2 E\{\chi^2\} \\ &\quad \cdot \sum_l \sum_k E\left\{ \alpha_{k,l}^2 \left(\int_{-\infty}^{\infty} q(t - T_l - \tau_{k,l}) r(t+\varepsilon) dt \right)^2 \right\} \\ &= K_D^2 \cdot A_t^2 A_r^2 \Omega_o E\{\chi^2\} \\ &\quad \cdot \sum_l \sum_k E\left\{ e^{-T_l/\Gamma} e^{-\tau_{k,l}/\gamma} \left(\int_{-\infty}^{\infty} q(t - T_l - \tau_{k,l}) r(t+\varepsilon) dt \right)^2 \right\} \end{aligned} \quad (12)$$

The loop gain of the tracking loop is a function of the received signal amplitude A_s. It is therefore desirable to have an Automatic Gain Controller (AGC) that precedes the tracking loop. The purpose of the AGC is to track the amplitude of the received monocycles to ensure constant loop gain and therefore a stable closed-loop error tracking loop. Here, we assumed a perfect AGC is deployed that multiplied the received signal with $\hat{A}_g$, which is the inverse of the estimated amplitude of the first ray in the l^{th} cluster to be tracked:

$$\hat{A}_g = e^{T_l/2\Gamma} \Big/ A_t \chi \sqrt{\Omega_o} \,. \quad (13)$$

And without lost of generality, we let $A_r = 1$. This implies that the noise variance at the input to the tracking loop has a modified one-sided power spectral density of:

$$N_o' = N_o E\{e^{T_l/\Gamma}\} \Big/ A_t^2 E\{\chi^2\} \Omega_o \,. \quad (14)$$

where $20\log_{10}(\chi)$ has a zero mean Gaussian distribution with variance σ_x^2.

The detector output variance while tracking the first ray of an arbitrarily cluster becomes:

$$K_D^2\left[\left(\int_{-\infty}^{\infty} q(t)r(t+\varepsilon)dt\right)^2 + \frac{E\{e^{T_l/\Gamma}\}}{A_t^2 E\{\chi^2\}\Omega_o}\cdot\frac{N_o}{2}\right] + K_D^2\sum_{k=1} E\left\{e^{-\tau_{k,l}/\gamma}\left(\int_{-\infty}^{\infty} q(t-\tau_{k,l})r(t+\varepsilon)dt\right)^2\right\}. \quad (15)$$

The variance expressed by (15) consists of two separate parts: variance of the first ray with AWGN and the variance attributed to self-interference from the multipath components.

IV. UWB Monocycle Model

In [1], we have modeled the received UWB monocycles as the n^{th} order ($n>0$) derivative of the Gaussian function. Its time and frequency domain representations are:

$$w_n(t) = (-1)^{\lfloor (3n+1)/2\rfloor} n!\,\pi^{-1/4} e^{-pt^2} \times \sum_{k=0}^{\lfloor n/2\rfloor} \frac{(-1)^k 2^{n+1/4-2k} p^{n/2+1/4-k} t^{n-2k}}{(n-2k)!k!\sqrt{(2n-1)!!}}. \quad (16)$$

$$W_n(f) = (-1)^n i^{n^2} \frac{(2\pi)^{n+\frac{1}{4}} p^{-\left(\frac{n}{2}+\frac{1}{4}\right)}}{\sqrt{(2n-1)!!}} f^n e^{-\pi^2 f^2/p}. \quad (17)$$

Here σ is a scaling factor that has the unit of time, $p=1/2\sigma^2$ and (2n-1)!!=(2n-1)(2n-3)…...3.1. The monocycle $w_n(t)$ has unit energy and the following properties: (a) For $n = even$, the maximum amplitude is at $t=0$ and positive. (b) For $n=odd$, the slope at $t=0$ is positive. (c) The monocycle satisfies $w_n(t) \approx 0$ for $|t| > T_D$. The parameter T_D is determined by σ and the order n. Increasing the derivative order has the effect of shifting the spectrum to occupy a higher frequency range. Maintaining the same energy per pulse, a larger scaling factor stretches the monocycle pulse wider in time and thus a more gradual rise of the main lobe of the waveform. The amplitude also has a role to play in defining the final shape of the monocycle waveform besides directly affecting the SNR.

In Fig. 2, we fit $w_4(t)$ to an empirically measured UWB impulse (with the amplitude at $t=0$ normalized to 1) obtained inside an anechoic chamber. The antenna used is a diamond dipole antenna. In Fig. 3, we fit the n-th order Gaussian derivative monocycle waveform to the FCC indoor limit to achieve maximum received signal energy by varying the order and scaling factor. A 'good' fit is chosen when σ minimizes the difference between $|W_n(f)|^2$ and the power limit defined by the FCC indoor spectral mask [8]. The result of the fitting is as shown in Fig. 3. In Fig. 4, the percentage of energy captured $\Phi = \int_{-k\sigma}^{k\sigma} w_n^2(t)dt \Big/ \int_{-\infty}^{\infty} w_n^2(t)dt$, by the correlator as we increase $T_D = k\sigma$ is illustrated. The quantity Φ characterizes the concentration of energy for monocycle of different order n as we integrate over a range further from the peak of the monocycle.

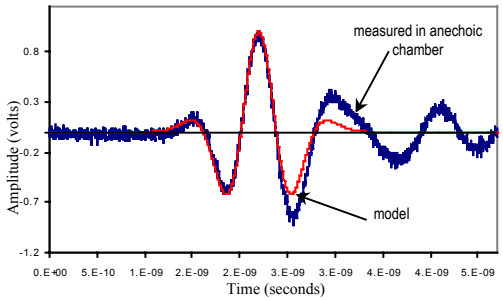

Figure 2: Comparison between experimentally measured and the analytic UWB monocycle. The signal is sampled at 2.5 pico-secs and σ =100 sample points or 2.5 x 10^{-10} seconds.

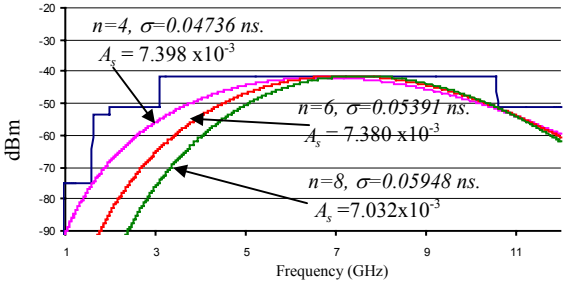

Figure 3: Fitting $w_4(t)$, $w_6(t)$ and $w_8(t)$ to the FCC indoor wireless spectral mask.

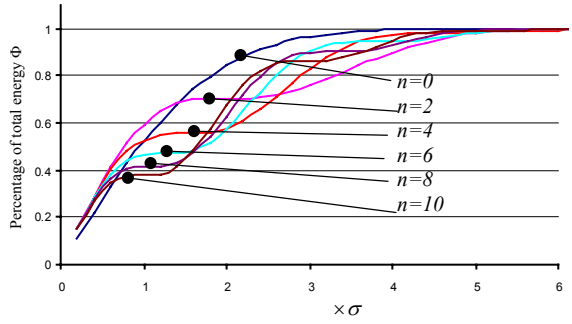

Figure 4: Percentage of total energy as a function of σ (two-sided) for UWB monocycle. We observed that for n=8, the width of the main lobe is about 1xσ and contains about 41% of the total energy.

V. CR Bound on Variance of First Ray

In the presence of additive noise, tracking the first ray of the cluster requires sufficient received signal energy for tolerable timing error jitter. This can be described by the Cramer-Rao (CR) lower bound, which has previously been derived in the radar community [5][6]. We follow the derivations in [6] and assuming a perfect AGC such that the input signal has a constant amplitude, the CR bound can be written as:

$$E\{\varepsilon^2\} \geq N_o' \big/ 2E_r\varpi^2 \quad (18)$$

where E_r is the received signal energy, $N_o' = (E\{e^{T_l/\Gamma}\}N_o)/(A_t^2 E\{\chi^2\}\Omega_o)$ and

$$\varpi^2 = \int \omega^2 \,|\, F(\omega)\,|^2 \, d\omega/(2\pi). \quad (19)$$

If $q(t) = w_n(t)$ then $\varpi^2 = (2n+1)p$. At 3 meters apart and assuming line-of-sight between transmitter and receiver, the

delay of the first ray of the first cluster is $T_0 \approx 10$ nsecs. If $\Gamma = 7.1$ [2], $e^{-T_l/\Gamma}$ can cause average tracking link margin of 6.1 dB $(= 10\log(e^{-10/7.1}))$.

VI. Analytical Expression for Multipath Variances

We postulate that, due to the narrow width of the UWB impulse, it is sufficient for most applications to consider only the variance due to the second ray of the cluster (assuming we are tracking the first ray of the cluster). In subsequent analysis, we let $q(t) = w_n(t)$ and $r(t) = w_m(t)$. Making use of the Parseval's relationship and the integral solutions in [7, 3.462], we arrive at:

$$\int_{-\infty}^{\infty} w_n(t-\tau_{k,l}) w_m(t+\varepsilon)dt = \frac{(-1)^{n+m}(n+m)!\,p^{(n+m)/2}e^{-\zeta^2 p/2}}{\sqrt{(2n-1)!!(2m-1)!!}} \sum_{k=0}^{\lfloor (n+m)/2 \rfloor} \frac{(-1)^k \zeta^{n+m-2k}}{(n+m-2k)!k!(2p)^k} \tag{20}$$

where $\zeta = \varepsilon + \tau_{k,l}$. If $\tau_{k,l} = 0$ and $\varepsilon = 0$, as $(n+m)$ is designed to be an odd number, (20) is identically zero.

If we are tracking the first ray in the cluster and neglecting effects of all other rays in the cluster besides the first and second rays, we have $\varepsilon = 0$ and $\tau_{k,l} = \tau_{1,l}$. Let V be the right-hand-side of (20), we have

$$V^2 = \frac{p^{n+m}\left((n+m)!\right)^2}{(2n-1)!!(2m-1)!!} \cdot \left\{ e^{-\tau^2 p} \sum_{v_1=0}^{\lfloor (n+m)/2 \rfloor} \frac{(-1)^{v_1}\tau^{n+m-2v_1}}{(n+m-2v_1)!v_1!(2p)^{v_1}} \sum_{v_2=0}^{\lfloor (n+m)/2 \rfloor} \frac{(-1)^{v_2}\tau^{n+m-2v_2}}{(n+m-2v_2)!v_2!(2p)^{v_2}} \right\}. \tag{21}$$

Therefore the variance due to the second ray of the cluster is

$$\sigma_\Delta^2 = K_D^2 \cdot E\left\{ V^2 e^{-\tau_{1,l}/\gamma} \right\} \tag{22}$$

and assuming a perfect AGC preceding the tracking loop, we have, from (2), (21) and (22) with $k = 1$:

$$\begin{aligned}\sigma_\Delta^2 = K_D^2 & \frac{\lambda p^{-1/2}\left((n+m)!\right)^2}{2^{n+m+1}(2n-1)!!(2m-1)!!} \\ & \times \sum_{v_1=0}^{\lfloor (n+m)/2 \rfloor} \sum_{v_2=0}^{\lfloor (n+m)/2 \rfloor} (-1)^{v_1+v_2} \cdot \exp\left\{ \frac{3(\lambda+1/\gamma)^2}{32p} \right\} \\ & \times \frac{(2(n+m)-2(v_1+v_2))!}{(n+m-2v_1)!v_1!(n+m-2v_2)v_2!} \\ & \times \left\{ \frac{\sqrt{\pi}}{\Gamma[(n+m)-(v_1+v_2)+1]} \cdot \right. \\ & {}_1F_1\left((n+m)-(v_1+v_2)+1/2; 1/2; \frac{(\lambda+1/\gamma)^2}{16p} \right) \\ & - \frac{\left(\sqrt{\pi/p}\right)\cdot(\lambda+1/\gamma)/2}{\Gamma[(n+m)-(v_1+v_2)+1/2]} \cdot \\ & \left. {}_1F_1\left((n+m)-(v_1+v_2)+1; 3/2; \frac{(\lambda+1/\gamma)^2}{16p} \right) \right\}\end{aligned} \tag{23}$$

where ${}_1F_1(\alpha;\gamma;z)$ is the confluent hypergeometric function. We have ignored the log-normal shadowing, Ω_o and the term $e^{-T_l/\Gamma}$ as they are common factors to all rays in the same cluster. They are assumed to be compensated by the Automatic Gain Controller (AGC) built into the tracking loop.

In Fig. 5, we plotted σ_Δ^2 as a function of $\lambda\sigma$ and γ/σ. The variance σ_Δ^2 can be interpreted as the timing error variance attributed to multipath in the channel. It is in additional to timing jitter contributed by other imperfections in the system such as AWGN and oscillator instabilities. It is evident that (23) correctly predicts that when $\lambda = 0$, $\sigma_\Delta^2 = 0$ and as $\gamma \to 0$, $\sigma_\Delta^2 \to 0$.

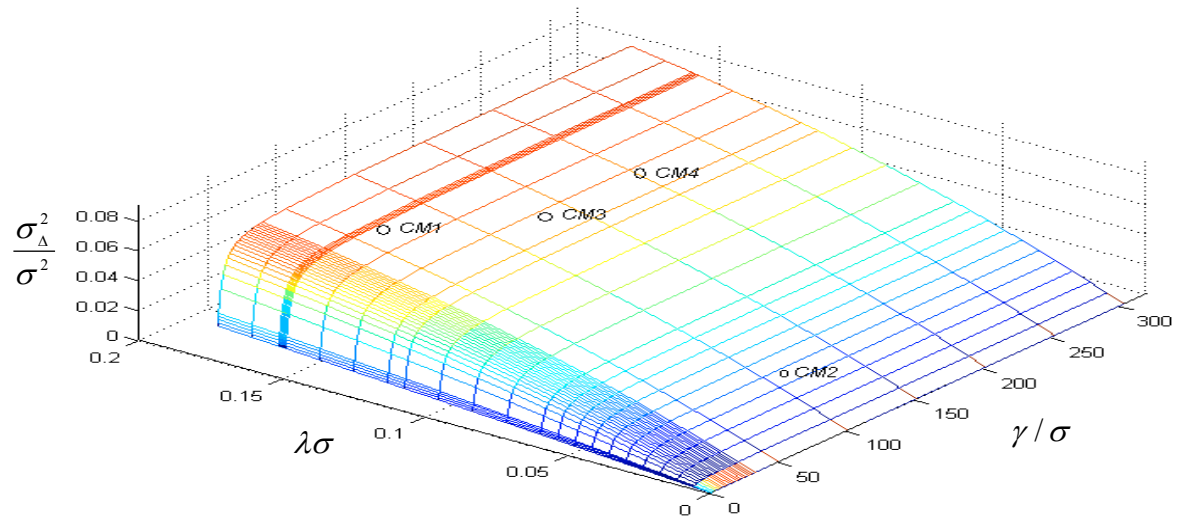

Figure 5: The additional variance σ_Δ^2 due to the 2nd ray of the cluster in a multipath propagation environment as a function of normalized quantities $\lambda\sigma$ and γ/σ. Here, we have let $A_t^2 A_r^2 \chi\Omega_o e^{-T_l/\Gamma} = 1$, $n=8$, $m=9$ and $\sigma = 0.05948$ ns.

VII. CHANNEL PARAMETERS AND OBSERVATIONS

In Table 1, the rate of arrival and attenuation for the four channel environments CM1, CM2, CM3 and CM4 described in [2] in relation to σ, which is a measure of the width of the monocycle waveform of (16) is listed. In Table 2, the standard deviation due to multipath translated to standard deviation in range ΔR as a result of σ_Δ^2 is tabulated.

It is of interest to note that the ratio $\sigma/(1/\lambda) = \sigma\lambda$ is a small quantity while γ/σ is relatively large for these channel environments. A large γ/σ puts the channel environment on the 'saturation' part of the σ_Δ^2 plot where σ_Δ^2 is not sensitive to variations in γ. As $1/\lambda$ is a measure of the temporal spacing of the multipaths and σ a measure of the width of the monocycles, a small $\sigma\lambda$ therefore indicates that the multipaths are likely to be resolved. This explains that for parameters given in [2], the additional standard deviation in range ΔR attributed to σ_Δ^2 is small and is less than half a centimeter.

In Fig. 5, we located approximately σ_Δ^2/σ^2 for the four channel environments CM1, CM2, CM3 and CM4 with *n=8* and $\sigma = 0.05948 ns$. The normalized variance σ_Δ^2/σ^2 has unit of sec^2/ sec^2. The small value of σ_Δ^2/σ^2 supports our proposition that we need only take into account the 2nd ray of the l^{th} multipath cluster when we considered multipath self-interference for most applications. In Fig. 6, we plotted σ_Δ^2 as we change the order of the reference monocycle assuming we are tracking the first ray. We noticed that as *m* increases, the S-function of the tracking loop becomes 'sharper' and σ_Δ^2 gets smaller. However, as pointed out in [1], the pull-in range of the tracking loop decreases as a result.

Table 1: Rate of arrival λ and attenuation γ in relation to monocycle waveform pulse width σ

		CM1	CM2	CM3	CM4
n=4 *σ=0.04736 (nsecs)*	λσ	0.12	0.024	0.099	0.0995
	γ/σ	90.79	141.47	166.81	253.38
n=6 *σ=0.05391 (nsecs)*	λσ	0.13	0.027	0.113	0.113
	γ/σ	79.76	124.28	146.54	222.59
n=8 *σ=0.05948 (nsecs)*	λσ	0.15	0.030	0.125	0.125
	γ/σ	72.29	112.64	132.82	201.7

Table 2: Additional standard deviation due to multipath for various channels where *n=8, m=9, σ*=0.05948 nsecs

	CM1 (LOS)	CM2 (No LOS)	CM3 (No LOS)	CM4 (No LOS)
σ_Δ (nsecs)	0.0162	0.0085	0.0154	0.0155
ΔR (meters)	0.0049	0.0025	0.0046	0.0046

Note: $\Delta R = \sigma_k K_k \cdot 3 \cdot 10^8$ is the standard deviation due to the 2nd ray in the multipath. Line-of-sight is denoted as LOS. We assume perfect AGC and tracking the first ray of an arbitrarily cluster.

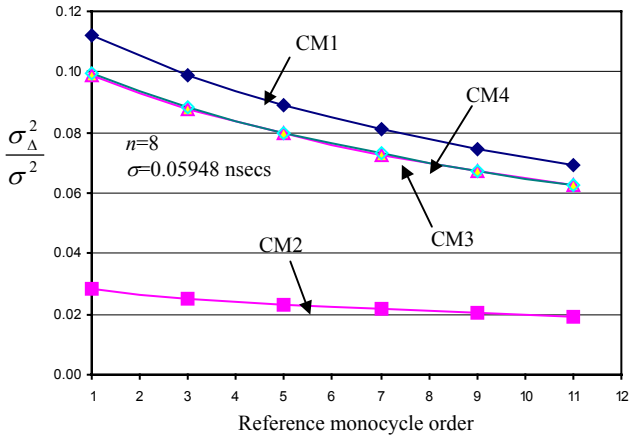

Figure 6: Variations of σ_Δ^2 for different *m*. Here *n=8* and $\sigma = 0.05948\ ns$.

VIII. CONCLUSIONS

We have examined the variance at the output of a timing detector meant for tracking UWB monocycle in an UWB multipath channel. The analysis suggests that, for channel parameters given in IEEE 802.15 report, the effects of multipath self-interference characterized by σ_Δ^2 on timing detector output may not be severe for UWB systems that optimize the spectral limits set by FCC indoor mask. However, the effect of fading on the CR bound should not be ignored. Lastly, we note that the received UWB monocycle model may not represent actual signals. However, $\lambda\sigma$ or ratio of effective pulse width for other UWB monocycle wave shape and ray arrival rate is likely to remain small for parameters recorded in [2] if the UWB monocycle optimizes the FCC allocated bandwidth, and our observations on multipath self-interference should hold.

REFERENCES

[1] Chee-Cheon Chui and Robert A. Scholtz, "Optimizing Tracking loop for UWB Monocycles", Globecom 2003.

[2] Jeff Foerster et. al., "Channel Modeling sub-committee Report Final", IEEE 802.15 Wireless Personal Area Networks, Nov. 18, 2002.

[3] Gunnar Fock, Jens Baltersee, Peter Schulz-Rittich and Henrich Meyr, "Channel Tracking for Rake Receivers in Closely Spaced Multipath Environments", IEEE Journal on Selected Areas in Communications, vol. 19, No. 12. December 2001.

[4] Peter Schulz-Rittich, Gunnar Fock, Jens Baltersee and Heinrich Meyr, "Low Complexity Adaptive Code Tracking with improved Multipath resolution for DS-CDMA communications over Fading channels", IEEE 6th Int. Sypm. on Spread-Spectrum Tech. & Appli., NJIT, Sept 6-8, 2000.

[5] Merrill I. Skolnik, *Introduction to Radar Systems*, 2nd Edition, McGraw-Hill, 1980.

[6] Harry L. Van Trees, *Detection, Estimation, and Modulation Theory: Part III – Radar-Sonar Signal Processing and Gaussian Signals in Noise*, Chapters 6.2, 9.2, 10.1 and 10.2, Wiley 1971.

[7] I. S. Gradshteyn & I.M. Ryzhik, *Table of Integrals, Series, and Products*, 5th Edition, equation 3.462, Academic Press, 1994.

[8] Federal Communications Commission, *Revision of Part 15 of the Commission's Rules Regarding Ultra-Wideband Transsmission Systems (ET Docket 98-153)*, April 2002.